DEVELOPMENT OF HARMONIC SUPPRESSED RECONFIGURABLE FRACTAL DIPOLE ANTENNA

SHIPUN ANUAR HAMZAH

A thesis submitted in fulfilment of the
requirements for the award of the degree of
Doctor of Philosophy (Electrical Engineering)

Faculty of Electrical Engineering
Universiti Teknologi Malaysia

JANUARY 2014

ABSTRACT

The development of compact size reconfigurable harmonic suppressed antenna is crucial in today's wireless communication system. One set of Harmonic Suppressed Antenna (HSA) and its reconfigurable configuration in the form of fractal dipole antenna that is integrated with the stubs and tapered balun has been designed and tested in this study. The Koch dipoles are double-sided structure while the tapered balun is triangular. Initial design is based on a 0.9GHz linear half-wavelength dipole. The Koch dipole antenna has equal arm lengths of 128mm. These are fabricated on a lossy FR-4 material. Printed fractal dipole antenna is designed to operate at 670MHz. This shows that the linear dipole can be miniaturized by employing Koch curve fractals onto the radiating structure. Fifteen bands reconfigurable antenna were designed to operate within 400MHz to 3.5GHz. However, as the frequency of operation is a low microwave band, the antenna physical size is relatively large. Tapered balun thus significantly enlarged the antenna size. In addition, the far field radiation pattern resembles that of a linear dipole. The overall antenna is found to be large and has moderate gain and efficiency. Nevertheless, it can potentially have higher gain and higher efficiency with the use of a low loss Rogers RT/Duroid material. Thus, the study on the reduction of the tapered balun size is worthwhile. Four sets of wideband tapered baluns with reduced sizes have been designed and tested as a matching circuitry in all the designed antennas. All baluns are found to perform well in terms of scattering parameters and power loss, despite having sizes of 25%, 50% and 75% smaller compared to the original structure. On the other hand, the feeding line method is also investigated. The first design takes into account of 38Ω input impedance of the fractal curve while the second design is a direct connection from the 50Ω SMA connector to terminal. The latter is then selected as it successfully eliminated the antenna's higher order modes, while the former is suitable for designing an optimum typical dipole antenna. Both antenna and balun are fabricated on Rogers 4530B. Four sets of HSA with reduced size have been designed and tested in this study. All sets were based on the 0.9GHz linear half-wavelength dipole and have equal arm lengths of 132mm. These are named as MFDB, MFDB75, MFDB50 and MFDB25. The antennas operate at 691MHz with low return loss and successfully suppressed their two harmonic frequencies. The MFDB25 antenna is found to exhibit similar performance in terms of the S-parameters and gain. It is also a compact antenna compared to the corresponding proposed HSA structure while the antenna achieved size reduction close to 19.7%, 31.4% and 43.4%. Hence, four sets of harmonic suppressed reconfigurable antennas named TMFDB, TMDB75, TMFDB50 and TMFDB25 have been designed and simulated. The total numbers of switches are 56, 54, 54, and 50 units respectively. TMFDB25 antenna is then fabricated and tested. It is found that the antenna has successfully configured 15 frequency bands and simultaneously suppressed higher order modes. The first prototype of an active TMFDB25 antenna is fabricated to enhance the performance. The suitability of this antenna for space–limited application of future communication system such as cognitive radio has been demonstrated. . The developed antenna can reduce the size of the front-end RF unit, reduce EMI interference and provide another additional characteristic for reconfigurable antenna. Hence the aim of this project has been achieved.

ABSTRAK

Pembangunan antena harmonik tertindas bolehkonfigursemula bersaiz padat adalah penting dalam sistem komunikasi tanpa wayar pada masa kini. Satu set Antena Harmonik Tertindas (HSA) dan bolehkonfigursemula dalam bentuk antena dwikutub fraktal yang diintegrasi dengan puntung dan balun tirus telah direka bentuk dan diuji. Dwikutub Koch adalah berstruktur sisi-dua manakala balun tirus berbentuk segitiga. Reka bentuk awal didasarkan kepada antena dwikutub linear separuh-panjang gelombang 0.9GHz. Antena Koch dwikutub mempunyai panjang lengan yang sama iaitu 128mm. Antena ini dihasilkan pada bahan berkehilangan tinggi FR-4. Antena tercetak dwikutub fraktal beroperasi pada 670MHz. Ini menunjukkan dwikutub linear boleh dikecilkan dengan ubah suaian struktur radiasi seperti Koch. Antena bolehkonfigursemula lima belas jalur kemudiannya direka bentuk untuk operasi julat 400MHz hingga 3.5GHz. Walau bagaimanapun, oleh kerana frekuensi operasi adalah jalur gelombang mikro rendah, saiz relatif fizikal antena adalah besar. Oleh itu, balun tirus meningkatkan saiz antena dengan ketara. Tambahan pula, corak sinarannya menyerupai dwikutub linear. Keseluruhan antena didapati besar dan mempunyai gandaan dan kecekapan sederhana. Namun, antena ini berpotensi mempunyai gandaan dan kecekapan yang boleh ditingkatkan dengan penggunaan bahan RT/Duroid kehilangan rendah. Maka, kajian terhadap pengurangan saiz balun tirus adalah bernilai. Empat set balun tirus jalur luas dengan pengecilan saiz telah direka bentuk dan diuji sebagai litar padanan antena. Prestasi semua balun adalah baik dari segi parameter serakan dan kehilangan kuasa walaupun bersaiz 25%, 50% dan 75% lebih kecil berbanding struktur asal. Selain itu, kaedah talian suapan turut dikaji. Reka bentuk pertama menggunakan galangan masukan 38Ω fraktal, manakala reka bentuk kedua bersambung terus dari penyambung SMA 50Ω ke terminal. Reka bentuk kedua dipilih kerana berjaya menghapuskan mod tertib tinggi antena, manakala reka bentuk pertama sesuai untuk antena dwikutub tipikal yang optimum. Antena dan balun dibina menggunakan Rogers 4350B. Empat set HSA dengan saiz yang dikurangkan telah direka bentuk dan diuji. Semua set adalah berasaskan antena dwikutub linear separuh-panjang gelombang 0.9GHz dan mempunyai panjang lengan yang sama iaitu 132mm. Antena dinamakan MFDB, MFDB75, MFDB50 dan MFDB25. Semua antena beroperasi pada 691MHz dengan kehilangan kembali rendah. Pada masa yang sama, ia berupaya menindas kedua-dua frekuensi harmonik. Antena MFDB25 didapati berprestasi serupa dari segi parameter–S dan gandaan. Ini menunjukkan bahawa ianya padat berbanding struktur cadangan HSA namun dengan pengurangan saiz menghampiri 19.7%, 31.4% dan 43.4%. Oleh itu, empat set antena harmonik tertindas bolehrekonfigursemula yang dipanggil TMFDB, TMDB75, TMFDB50 dan TMFDB25 telah direka bentuk dan disimulasi. Jumlah suis masing-masing ialah 56, 54, 54 dan 50 unit. Antena TMFDB25 kemudian dibina dan diuji. Didapati ia berjaya mengkonfigurasi mana-mana 15 jalur frekuensi dan menyekat mod tertib tinggi secara serentak. Prototaip pertama antena aktif TMFDB25 dibina untuk peningkatan prestasi. Kesesuaian antena TMFDB25 bagi aplikasi terhad ruang untuk sistem komunikasi di masa hadapan seperti radio kognitif telah ditunjukkan. Penghasilan antena ini dapat mengecilkan saiz unit bahagian depan RF, merendahkan ganguan EMI dan menambahkan satu ciri tambahan antena bolehkonfigursemula. Justeru, objektif projek ini telah dicapai.

TABLE OF CONTENTS

CHAPTER	TITLE	PAGE
	DECLARATION	ii
	DEDICATION	iii
	ACKNOWLEDGEMENTS	iv
	ABSTRACT	vi
	ABSTRAK	vii
	TABLE OF CONTENTS	viii
	LIST OF TABLES	xii
	LIST OF FIGURES	xiv
	LIST OF ABBREVIATIONS	xxiii
	LIST OF SYMBOLS	xxvi
	LIST OF APPENDICES	xxviii
1	**INTRODUCTION**	**1**
	1.1 Background	1
	1.2 Problem Statement	2
	1.3 Research Objective	3
	1.4 Research Scopes	4
	1.5 Significance of Research Contribution	5
	1.6 Organization of the Thesis	7
2	**LITERATURE REVIEW**	**8**
	2.1 Review of Reconfigurable Antenna	10

	2.1.1	The State of the Art in Antenna Design for the user Terminal	11
	2.1.2	Small Element "Modern" Tunable Antenna	12
	2.1.3	Tune-ability Technique	16
2.2	Review of Fractal Antenna		19
	2.2.1	Koch curve properties	22
	2.1.2	Reconfigurable fractal antenna	24
2.3	Review of Antenna Miniaturization		26
2.4	Review on the balun circuit		30
2.5	Review of Harmonic Suppressed Antennas		35
2.6	Current and Previous Research		39
2.7	Summary		41
3	**RESEARCH METHODOLOGY**		**42**
3.1	Introduction		44
3.2	Design methodology		45
3.3	Typical tapered balun and its miniaturized proposed structure		49
3.4	Simulation set up		53
3.5	Measurement environment set up		54
3.6	Design the prototype antenna		58
3.7	Validation work		64
3.8	Summary		65
4	**DESIGN AND DEVELOP FRACTAL DIPOLE ANTENNA WITH TAPERED BALUN**		**66**
4.1	Design of tapered balun		67
4.2	Fractal dipole antenna with tapered balun structure		72
4.3	Antenna geometries and design procedures		75
4.4	Higher order modes		79
4.5	Results		82
	4.5.1	Design 1	82

	4.5.2	Design 2	87
4.6	Summary		91
5	**HARMONIC SUPPRESSED FRACTAL DIPOLE ANTENNA**		**92**
5.1	Introduction		93
5.2	Antenna Design with Harmonic Filter		93
	5.2.1	Antenna Design Structure	94
	5.2.2	Antenna Optimization	98
	5.2.3	Antenna Size Reduction and Characteristics	101
	5.2.4	Prototypes	105
5.3	Experimental Results		106
	5.3.1	Prototype of MFDB Antenna	106
	5.3.2	Prototype of MFDB75 Antenna	116
	5.3.3	Prototype of MFDB50 Antenna	119
	5.4.3	Prototype of MFDB25 Antenna	121
5.4	Summary		131
6	**HARMONIC SUPPRESSED RECONFIGURABLE FRACTAL DIPOLE ANTENNA**		**132**
6.1	Introduction		134
6.2	Antenna Design Structure		136
6.3	Simulation and Experimental Results of TMFDB Antenna		143
	6.3.1	TMFDB Antenna	144
	6.3.2	TMFDB75 Antenna	146
	6.3.3	TMFDB50 Antenna	148
	6.3.4	TMFDB25 Antenna Prototype	149
6.4	Performance comparison		171
6.5	TMFDB25 antenna using RF pin diodes		173
	6.5.1	Simulation results	175
	6.5.2	Measurement results	176
6.6	Summary		181

7	**CONCLUSION**	**182**
	7.1 Conclusion	184
	7.2 Recommendation for future work	187
REFERENCES		**186**
Appendices A – F		196-249

LIST OF TABLES

TABLE NO.	TITLE	PAGE
2.1	Reconfigurable printed antenna	18
2.2	Reconfigurable fractal antenna	26
2.3	Selected tapered balun	33
2.4	Selected HSAs	38
3.1	Antenna specification for a hand held unit system	47
3.2	Reconfigurable antenna conditions	63
4.1	Simulated results of the designed baluns using CST	69
4.2	Simulated results of the designed baluns using HFSS	71
4.3	Measurement works of the designed baluns	72
5.1	Simulated Return Losses of harmonic suppressed fractal dipole antenna with different iteration number. NA: not available	98
5.2	Effect of terminal length, *L*, on resonance in Figure 5.2.	99
5.3	Effect of stub-filter's length on resonance in Figure 5.2 is location of stub 2 with respect to stub 1.	99
5.4	Effect of stub-filter's width on resonance in Figure 5.2.	99
5.5	MFDB with stubs performance characteristic at operating frequency, *f*	104
5.6	MFDB with stubs performance characteristic at *1st HM*	104
5.7	MFDB with stubs performance characteristic at 2nd *HM*	105
5.8	Optimized dimensions of the MFDB antenna	107
5.9	Measured and Simulated Frequencies, RL and VSWR at f, 1st HM and 2nd HM	109
5.10	Simulated and measured gain of the proposed MFDB antenna	114
5.11	Measured voltages of the MFDB antenna	115

5.12	Simulated and measured gain of the proposed MFDB75 antenna	118
5.13	Measured voltages of the MFDB75 antenna	118
5.14	Simulated and measured gain of the proposed MFDB50 antenna	121
5.15	Measured voltages of the MFDB50 antenna	121
5.16	Optimized dimensions of the MFDB25 antenna	122
5.17	Simulated and measured frequencies, RL and VSWR at f, 1st HM and 2nd HM	124
5.18	Simulated and measured gain of the proposed MFDB25 antenna	131
5.19	Measured voltages received of the MFDB25 antenna	131
6.1	Variation of *L* and the corresponding switch condition states	138
6.2	Summary of the stubs – filter lengths	139
6.3	Discrete radiating elements and stubs lengths, as shown in Figure 6.3 for selected antenna operating frequencies	140
6.4	Frequency reconfigurable antenna performance	146
6.5	Return Losses of the theoretical predictions versus measurement for TMFDB25 antenna	166
6.6	VSWR of the theoretical predictions versus measurement for TMFDB25 antenna	167
6.8	Antenna Dimensions. Unit is in mm.	174
7.1	Performance comparison of HSA	185
7.2	Performance comparison of frequency reconfigurable antennas	186
7.3	Performance comparison of frequency reconfigurable active antennas	186

LIST OF FIGURES

FIGURE NO.	TITLE	PAGE
2.1	Reconfigurable dipole antenna (a) printed dipole using pin diode [23], and (b) printed dipole using MEMS switches [24]	13
2.2	Frequency reconfigurable dipole (a) [25] using linear dipole (b) [26] using a folded dipole, and (c) [27] using a vee-dipole.	14
2.3	Harmonic suppressed reconfigurable dipole antenna (a) [17] using a linear dipole and (b) log periodic antenna [28]. The ideal switch is used to connect or disconnect the radiating element and harmonic trap.	15
2.4	(a) Tapered balun, and (b) Input Impedance, $Z_{in\text{-}antenna}$ of printed Koch dipole antenna	21
2.5	Fractal Koch's geometries construction [54]	22
2.6	Block diagram of the IFS [54]	23
2.7	Typical fractal curve. (a) the first four iterations in the construction of a stand Koch curve, (b) the first four stages in the construction of a Hilbert curve, and (c) the four stages in the construction of Sierpinski Carpet curve.	25
2.8	(a)-(b) Photograph of a miniature GA optimized Koch fractal dipole antenna with balun, (c) miniature credit-card-size 916 MHz AM transmitter with components directly written on glass including a miniature meander-line dipole antenna [71]–[72]	29
2.9	Two miniaturized antennas using fractal curve. (a) Miskowski fractal (1st iteration) (left) and square antenna (right) with bazooka balun, and (b) rectangular patch antenna (left) and	

	non-square fractal patch (right) operate at 5.2 GHz. [60]	30
2.10	A typical schematic for a balanced to unbalanced structure [82]	31
2.11	Unbalanced-to-balanced connected back-to-back [86]	32
2.12	Tapered balun integrated with the load, *R*	32
2.13	Transition configurations with size reduction [73]. (a) Microstrip – broadside parallel strip line tapered balun with bend of 90°, (b) Microstrip – CPS transition tapered balun with bend of 90°Unbalanced-to-balanced connected back-to-back [86]	34
2.14	Dipole with harmonic suppressed [74]	35
2.15	Wideband Reconfigurable Slot Antenna (the black colour is the conductor while the grey colour is non conductor) [12]	40
2.16	Switchable two-port wideband circular antenna [13].	40
2.17	Wide-narrowband antenna [14]. (a) top view, and (b) bottom view. The grey colour is the conductor on the top layer while the dash line is the conductor on the bottom layer.	41
2.18	Switchable vivaldi antenna [15]	42
3.1	Flow chart of the research methodology	46
3.2	Tunable single microwave band in a time (*note:* black = active channel; white = non-active channel)	47
3.3	Basic geometry of the proposed single band fractal dipole antenna with tapered balun; (a) front-view and (b) side-view.	48
3.4	Layout of microstrip tapered balun (a) front side of substrate, and (b) back side. The dimensions are X = 33 mm, V_1 = 137 mm, V_2 = 3.42 mm, W_2 = 33 mm, and W_1 = 3.42 mm.	49
3.5	Tapered balun design procedure: microstrip-to-DSPSL transition (a) the top layer and (b) the bottom layer	52
3.6	Layout of the semi anechoic chamber	56
3.7	Set up for antenna pattern measurement	56
3.8	(a) E-plane (ZX plane) and gain measurement setup (coordinate) for antenna in this chapter, and (b) H-plane (XZ-plane) measurement setup (coordinate) for antenna.	57
3.9	(a) Frequency domain (power received of AUT) antenna	

	measurement set-up, and (b) the photograph of the power received measurement setup.	58
3.10	Koch curve geometry with indentation angle and predicted length	59
3.11	Side view of microstrip transmission line for matching circuitry	60
3.12	Cross section of a parallel strip line	60
3.13	The complete design of a tunable fractal dipole antenna (a) top view, (b) bottom view and (c) side view	62
4.1	(a) Geometry of a fractal dipole antenna with $n = 0$. (b) Simulated $\|S_{11}\|$ response of the antenna for varying W.	73
4.2	(a) Geometry of a fractal dipole antenna with $n = 1$. (b) Simulated $\|S_{11}\|$ of the antenna when W is changed to 2.0 mm, 2.5 mm, 3.0 mm, 3.5 mm, and 4.0 mm.	74
4.3	(a) Geometry of a fractal dipole antenna with $n = 2$. (b) Simulated $\|S_{11}\|$ of the antenna when W is changed to 2.0 mm, 2.5 mm, 3.0 mm, 3.5 mm, and 4.0 mm.	74
4.4	(a) Geometry of a fractal dipole antenna with $n = 3$. (b) Simulated $\|S_{11}\|$ of the antenna when W is changed to 2.0 mm, 2.5 mm, 3.0 mm, 3.5 mm, and 4.0 mm.	75
4.5	Geometry of the printed Fractal dipole antenna with $W = 3.8$ mm, and $H = 66$ mm as a reference.	76
4.6	Proposed antenna prototypes with the top layer, and bottom layer. (a) Antenna 1a_*W* (*H* original), (b) Antenna 2a _*W* (*H* 25% reduction), (c) Antenna 3a_*W* (*H* 50% reduction), and (d) Antenna 4a_*W* (*H* 75% reduction)	78
4.7	Proposed antenna prototypes with the top layer, and bottom. (a) Antenna 1b_*W* (*H* original), (b) Antenna 2b_*W* (*H* 25% reduction), (c) Antenna 3b_*W* (*H* 50% reduction), and (d) Antenna 4b_*W* (*H* 75% reduction)	79
4.8	Measured return loss of a printed dipole antenna	80
4.9	Measured return loss of printed fractal dipole antenna	82
4.10	Measured input return loss ($\|S_{11}\|$) and voltage standing wave	

	ratio ($\|VSWR\|$) at the first operating frequency, f_1.	84
4.11	Measured radiation patterns at the operating frequency, f_1 of (a) Antenna 1a, (b) Antenna 2a, (c) Antenna 3a, and (d) Antenna 4a.	86
4.12	Measured input return loss ($\|S_{11}\|$) and voltage standing wave ratio ($\|VSWR\|$) at the first operating frequency, f_1.	89
4.13	Measured radiation pattern at the operating frequency, f_1 of (a) Antenna 1b, (b) Antenna 2b, (c) Antenna 3b, and (d) Antenna 4b.	91
5.1	Proposed single band antenna design. (a) RF front-end with multiband Koch dipole antenna (n = 1) and harmonic filter, and (b) Proposed single band Koch dipole antenna with stub	94
5.2	Geometry of the printed fractal dipole antenna that operates at 725MHz (a) MFD antenna, (b) MFD with terminal using a strip line, and (c) MFDB antenna with stub 1 and with stubs 1, 2	95
5.3	Photographs of MFDB antenna, (a) front view, (b) back view	107
5.4	Simulated and measured return losses of the MFDB antenna, at three conditions: (i) MFDB without stub, (ii) MFDB with stub1, and (iii) MFDB with stubs 1, 2.	108
5.5	Simulated and measured VSWRs of the MFDB antenna	108
5.6	(a) MFDB antenna without stubs, (b) surface current distribution, (c) return loss, and (d) Conceptual equivalent circuit	110
5.7	(a) MFDB antenna with stub 1, (b) surface current distribution, (c) return loss, amd (d) Conceptual equivalent circuit	110
5.8	(a) MFDB antenna with stubs 1,2 , (b) surface current distribution, (c) return loss, amd (d) Conceptual equivalent circuit	111
5.9	Measured E–Plane radiation pattern at 691 MHz for three cases: (i) MFDB without stubs, (ii) MFDB with stub 1,	

	and (iii) MFDB with stubs 1, 2.	112
5.10	Measured H–Plane radiation pattern at 691 MHz for three cases: (i) MFDB without stubs, (ii) MFDB with stub 1, and (iii) MFDB with stubs 1,	112
5.11	Measured E–Plane radiation pattern at 1st HM of 1969 MHz for three cases: (i) MFDB without stubs, (ii) MFDB with stub 1, and (iii) MFDB with stubs 1, 2	113
5.12	Measured H–Plane radiation pattern at 1969 MHz for three cases: (i) MFDB without stubs, (ii) MFDB with stub 1, and (iii) MFDB with stubs 1, 2	113
5.13	Measured E–Plane radiation pattern at 3200 MHz and 2900 MHz for three cases: (i) MFDB without stubs, (ii) MFDB with stub 1, and (iii) MFDB with stubs 1, 2	114
5.14	Photographs of MFDB75 antenna. (a) Front view, (b) Back view	116
5.15	Simulated and measured return losses of MFDB75 antenna.	117
5.16	Simulated and measured VSWR of MFDB75 antenna.	117
5.17	Photographs of MFDB50 antenna. (a) Front view. (b) Back view	119
5.18	Simulated and measured return losses of MFDB50 antenna.	120
5.19	Simulated and measured VSWR of MFDB50 antenna	120
5.20	Top (a) and bottom (b) views of the fabricated MFDB25 antenna	122
5.21	Measured and simulated return losses of the MFDB25, at three conditions: (1) without stub, (2) with stub1 and (3) with stubs 1, 2.	123
5.22	Simulated and measured VSWR of the MFDB25 antenna	124
5.23	(a) MFDB25 antenna without stubs, (b) surface current distribution, (c) return loss, and (d) Conceptual equivalent circuit	125
5.24	(a) MFDB25 antenna with stub 1, (b) surface current distribution, (c) return loss, and (d) Conceptual equivalent circuit	125
5.25	(a) MFDB25 antenna with stubs 1,2 , (b) surface current	

	distribution, (c) return loss, and (d) Conceptual equivalent circuit	126
5.26	Realized gain patterns of the MFDB25 antenna in the passband mode and stopband mode. (a) Perspective view of the antenna without stubs (top) and perspective view of the antenna with stubs (bottom) in spherical coordinates system, (b) resonant frequency (without stubs), 740 MHz (1.85 dB) and resonant frequency (with stubs), 740 MHz (1.73 dB), (c) 1st HM (without stubs) (3.78 dB) and 1st HM (with stubs) (~-1.0 dB), and (d) 2nd HM (without stubs) (4.78 dB), and 2nd HM (with stubs) (~-8.0 dB).	127
5.27	Measured E-plane radiation pattern at 691 MHz for three cases: (i) MFDB25 without stubs, (ii) MFDB25 with stub 1, and (iii) MFDB25 with stubs 1, 2.	128
5.28	Measured H-plane radiation pattern at 691 MHz for three cases: (i) MFDB25 without stubs, (ii) MFDB25 with stub 1, and (iii) MFDB25 with stubs 1, 2	128
5.29	Measured E-plane radiation pattern at 1969 MHz for three cases: (i) MFDB25 without stubs, (ii) MFDB25 with stub 1, and (iii) MFDB25 with stubs 1, 2	129
5.30	Measured H-plane radiation pattern at 1969 MHz for three cases: (i) MFDB25 without stubs, (ii) MFDB25 with stub 1, and (iii) MFDB25 with stubs 1, 2	129
5.31	Measured E-plane radiation pattern at 3010 MHz for three cases: (i) MFDB25 without stubs, (ii) MFDB25 with stub 1, and (iii) MFDB25 with stubs 1, 2	130
5.32	Measured H-plane radiation pattern at 3010 MHz for three cases: (i) MFDB25 without stubs, (ii) MFDB25 with stub 1, and (iii) MFDB25 with stubs 1, 2	131
6.1	Proposed tunable MFDB antenna conceptual (a) RF front-end with fractal dipole antenna (n = 2) and tunable harmonic filter (b) Proposed tunable single band fractal dipole antenna with stubs	135
6.2	Geometry of the reconfigurable MFDB antenna that operates at 741 MHz.	137

6.3	Reconfigurable MFDB antenna (of half arm) with stub-filter, balun and RF switch locations	138
6.4	Reconfigurable TMFDB active layer (radiating element's length, Ln) switch configuration states. Switches in ON position are shown in black, switches in OFF position are shown in grey. The lengths are tabulated in Table 6.3.	139
6.5	Open circuit stubs (stubs-filter) configuration states. Switches is ON position are shown in black, switches in OFF position are shown in grey.	141
6.6	Reconfigurable MFDB antenna and RF switch locations (a) original size, (b) TMFDB75, (c) TMFDB50, and (d) TMFDB25 antenna. Units are in mm.	142
6.7	Geometry of the tuning parallel stubs for the reconfigurable antenna	143
6.8	Simulated tunable return losses of TMFDB antenna using CST (a) with higher order modes, and (b) with suppressed higher order modes	145
6.9	Simulated tunable Return losses of TMFDB75 antenna using CST (a) with higher order modes, and (b) with suppressed higher order modes	147
6.10	Simulated tunable Return losses of TMFDB50 antenna using CST (a) with higher order modes, and (b) with suppressed higher order Modes	149
6.11	Geometry of TMFDB25 antenna with 50 switches in OFF condition with top view (left side), bottom view (right side), and side view.	150
6.12	Geometry of TMFDB25 antenna with switches operates at Band 1, 740 MHz	151
6.13	Prototype of TMFDB25 antenna with switches operate at Band 1, 691 MHz	151
6.14	Simulated tunable return losses of (a) TMFDB25 antenna with higher order modes using CST, and (b) TMFDB25 antenna with suppressed higher order modes using CST	153
6.15	Simulated E-plane and H-plane radiation patterns of	

	Bands 1, 2, 3, 4, and 5 using CST	154
6.16	Simulated E-plane and H-plane radiation patterns of Bands 6, 7, 8, 9, and 10 using CST	155
6.17	Simulated E-plane and H-plane radiation pattern of bands 11, 12, 13, 14, and 15 using CST	155
6.18	Simulated tunable return losses of (a) TMFDB25 antenna with higher order modes using HFSS, and (b) TMFDB25 antenna with suppressed higher order modes using HFSS	157
6.19	Simulated E-plane and H-plane radiation patterns of Bands 1 to 5 using HFSS	158
6.20	Simulated E-plane and H-plane radiation patterns of Bands 6 to 10 using HFSS	158
6.21	Simulated E-plane and H-plane radiation patterns of Bands 11 to 15 using HFSS	159
6.22	Tunable return losses for bands 1, 3, 5, 7, and 9 with suppressed higher modes	160
6.23	Tunable return losses for bands 2, 4, 6, 8, and 10 with suppressed higher modes	161
6.24	Tunable return losses for bands 11, 12, 13, 14, and 15 with suppressed higher modes	161
6.25	Measured E–Plane radiation pattern (co-polar & cross-polar) at operating frequency, f, for TMFDB with stubs 1, 2 at band 1, band 2, band 3, band 4, and band 5.	163
6.26	Measured H–Plane radiation pattern (co-polar & cross-polar) at operating frequency, f, for TMFDB with stubs 1, 2 at bands 1 to 5	163
6.27	Measured E–Plane radiation pattern (co-polar & cross-polar) at operating frequency, f, for TMFDB with stubs 1, 2 at bands 6 to 10	164
6.28	Measured H – Plane radiation pattern (co-polar & cross-polar) at operating frequency, f, for TMFDB with stubs 1, 2 at bands 6 to 10	164
6.29	Measured E–Plane radiation pattern (co-polar & cross-polar) at operating frequency, f, for TMFDB at bands 11 to 15.	165

6.30	Measured H–Plane radiation pattern (co-polar & cross-polar) at operating frequency, f, for TMFDB at bands 11 to 15.	165
6.31	Simulated realized gain of TMFDB25 antenna using CST and HFSS	168
6.32	Simulated surface current distribution of the TMFDB25 antenna. (a) bands 1 to 4, (b) bands 5 to 8, (c) bands 9 to 12, (d) bands 13 to 15 in Figure 6.6(d).	169
6.33	Realized gain response of the proposed TMFDB25 antenna at the operating frequency, 1st HM and the 2nd HM	170
6.34	Total Efficiency response of the proposed TMFDB25 antenna at the 1st HM and 2nd HM	170
6.35	Simulated realized gain of TMFDB25 antenna with suppressed higher order modes	172
6.36	Simulated efficiency of TMFDB25 antenna with suppressed higher order modes	172
6.37	Geometry of TMFDB25 antenna (a) without stub, (b) with stub, (c) side view, (d) top view, and (e) spherical coordinate systems	174
6.38	Simulated reconfigurable S_{11} with higher order modes of active TMFDB25 antenna	175
6.39	Simulated reconfigurable S_{11} with suppressed higher order modes of active TMDB25 Antenna	176
6.40	Photograph of the proposed antenna with bias circuit	177
6.41	Measured reconfigurable S_{11} with HMs of the proposed antenna	179
6.42	Measured reconfigurable S_{11} with suppressed HMs of the proposed antenna	180
6.43	Measured radiation pattern. (a) Band 1 excited at 1.1 GHz, E-plane (blue colour), H-plane (red colour). (b) Band 2 exited at 2.2 GHz, E-plane (blue colour) , H-plane (red colour)	181
6.44	Measured radiation pattern. (i) Band 3 excited at 3.1 GHz E-plane (blue colour), H-plane (red colour). (ii) Band 4 at 2.0 GHz, E-plane (blue colour), H-plane (red colour).	182

LIST OF ABBREVIATIONS

CR	-	Cognitive radio
TV spectrum	-	Television spectrum
HSA	-	Harmonic suppressed antenna
AIA	-	Active integrated microwave antenna
RECTENNA	-	Rectifier antenna
RF	-	Radio frequency
EMI	-	Electromagnetic interference
GSM	-	Global system for mobile communication
ISM	-	Industrial, Scientific and Medical
3G	-	Third generation
LPF	-	Low pass filter
MFD	-	Miniaturized fractal dipole
MFDB	-	Miniaturized fractal dipole with balun1b
MFDB75	-	Miniaturized fractal dipole with balun2b
MFDB50	-	Miniaturized fractal dipole with balun3b
MFDB25	-	Miniaturized fractal dipole with balun4b
TMFDB	-	Tunable miniaturized fractal dipole with balun1b
TMFDB75	-	Tunable miniaturized fractal dipole with balun2b
TMFDB50	-	Tunable miniaturized fractal dipole with balun3b
TMFDB25	-	Tunable miniaturized fractal dipole with balun4b
FR-4	-	Fire resistant-4
DC	-	Direct current
AC	-	Alternating current
TEM	-	Transverse electromagnetic
DSPSL	-	Double-sided parallel strip line
E-Plane	-	Electric plane
H–Plane	-	Magnetic plane

SCS	-	Spherical coordinate system
3-D	-	Three dimensional
HPBW	-	Half-power bandwidth
SMA	-	miniaturized version A
CR/SDR	-	Cognitive radio/Software defined radio
QoS	-	Quality of services
UHF band	-	Ultra high frequency band
CI	-	Computational Intelligent
FPGA	-	Field programmable gate array
Tx/Rx	-	Transmitter/ Receiver
PIFA	-	Planar inverted-F antenna
LPDA	-	Log periodic dipole antenna
MEMS	-	Micro-electromechanical
GaAs FET	-	Gallium arsenide field effect transistor
WWAN	-	Wireless wide area network
WLAN	-	Wireless local area network
UWB	-	Ultra wideband
CPW	-	Coplanar waveguide
LTCC	-	Low temperature co-fired ceramic
GA	-	Genetic algorithm
VSWR	-	Voltage standing wave ratio
EBG	-	Electromagnetic bandgap
DGS	-	Defected ground structure
PBG	-	Photonic bandgap
DMS	-	Defected microstrip structure
CST	-	Computer simulation technology
HFSS	-	High frequency structure simulator
FD	-	Frequency domain
RHSA	-	Reconfigurable harmonic suppressed antenna
EMC	-	Electromagnetic Compatibility Centre
FeCl	-	Ferric chloride
AUT	-	Antenna under test
LOS	-	Line of Sight
FEM	-	Finite element method

FIT	-	Finite integration method
dB	-	Decibel
%BW	-	Percentage bandwidth
RLC	-	Resistor-Inductor-Capacitor
UTHM	-	Universiti Tun Hussein Onn Malaysia
Balun1b	-	Balun with original size
Balun2b	-	Balun with 25% size reduction
Balun3b	-	Balun with 50% size reduction
Balun4b	-	Balun with 75% size reduction
Mag. Z	-	Magnitude of impedance

LIST OF SYMBOLS

λ	-	Wavelength
c	-	Speed of light
f	-	Frequency
Z_g	-	Serial impedance
Z_c	-	Characteristic impedance
R_L	-	Loss resistance
R_r	-	Radiation resistance
X_A	-	Reactance
Z_o	-	Characteristic impedance
h	-	Substrate height
w	-	Line width
ε_r	-	Dielectric constant
ε_{reff}	-	Effective dielectric constant
λ_g	-	Effective wavelength
l_t	-	Taper matching ciruit of length
R	-	Resistor
C	-	Capacitor
l_T	-	Predicted length of the koch dipole
n	-	Iteration number
$f_{n=0}$	-	Initial first resonance ($n = 0$)
D	-	Fractal antenna dimension
H_{balun}	-	Height of balun
W_{balun}	-	Width of balun
1st HM	-	First higher order mode
2nd HM	-	Second higher order mode

3rd HM	-	Third higher order mode
HM	-	Higher order mode
R_{in}	-	Input resistance of Koch curve
R_{in0}	-	Input resistance of a linear dipole
$\|S_{11}\|$	-	Magnitude of reflection coefficient
$\|S_{21}\|$	-	Magnitude of insertion loss
R*r*	-	Radiation resistance
W	-	Ground plane width
t	-	Copper thickness
Lp	-	Parasitic element length
s	-	Sub-parasitic element
g	-	Gap separating the adjacent section of the sub-parasitic element
Z_1	-	Reactive load 1
Z_2	-	Reactive load 2

LIST OF APPENDICES

APPENDIX	TITLE	PAGE
A	List of the equipments and the measurement works	197
B1	The simulation results of the balun in Chapter 3	222
B2	Active antenna design and simulation method in Chapter 3	228
C	Simulation and measurement results of back-to-back configuration in Chapter 3	232
D	S-Parameters simulation results in Chapter 5	238
E1	Simulation and measurement results of TMFDB25 in Chapter 6	242
E2	3-D radiation patterns of active TMFDB25	244
F	Publications during the doctorate study	246

CHAPTER 1

INTRODUCTION

1.1 Background

The electromagnetic radio spectrum is one of the most essential natural resources nowadays. Conversely, access to this spectrum is complex and difficult with the existing regulatory framework. This problem has alerted researches to investigate the revolutionary technique such as cognitive radio (CR) for efficient frequency management. Recently, the system has been introduced as a new feature for radio communication system such as mobile handset unit [1]. This will allow users to share the spectrum frequency, allocated from other sources such as unused TV spectrums. To fulfill the application, a new technique known as reconfigurable narrowband to narrowband has been developed [2]-[6]. In addition, a narrowband to narrowband with harmonic suppression capability is incorporated to the design for the most optimum antenna performance. Frequency, radiation pattern or polarization can be organized by means of reconfigurable antenna. In order to design an antenna with this new feature, the harmonic suppressed antenna (HSA) is initially designed. The antenna is also useful in an active integrated microwave antenna (AIA), active antenna array and rectifying antenna (RECTENNA) system. There are varieties of HSA that are capable for suppressing unwanted harmonic frequencies such as in [7]-[11]. The harmonic suppressed antenna and its reconfigurable configuration offers major benefit such as simplifying the radio frequency (RF) front-end circuit, reduce

electromagnetic interference (EMI) and overcome antenna limited space problem. Hence, this avoids overlapping of operating frequency and the higher order modes, since a single band is used at a time i.e. suppression of the higher order mode. Other new variations of frequency reconfigurable antennas have also received attention which recommend multi-functionality as the primary objective to cater CR radio applications [12]-[16]. Harmonic suppressed narrowband to narrowband antenna employs fractal technology that offers a compact size, multi-mode application that operates in the TV band, GSM band, ISM band, or 3G band. This antenna has been identified as one of the main candidates for future wireless communication that incorporates wide spectrum sensing to resolve the unused RF spectrum allocation and frequency agile RF front-ends unit for RF communication systems.

1.2 Problem Statement

The application of harmonic suppressed feature in an reconfigurable antenna is getting an attractive attention since it is producing a unique operation and practical in size.

The double-sided printed antenna proposed by A. Mirkamali *et al.* (2006) [17] is basically suitable for handheld user terminal applications. The configuration allows the antenna to trap the higher order mode. It can select seven frequency bands from 0.9 GHz to 3.0 GHz with omni-directional radiation pattern. However, it is not clear how this type of antenna can produce single frequency band. Moreover, the feeding circuit operation resulted in a large size antenna operating at low frequency band. There is an immediate need to reduce the antenna size, develop an equivalent circuit and enhance the overall performance.

Reconfigurable harmonic suppressed fractal antenna is useful to reduce the overall antenna size and to add new feature to a terminal that operates in a multi-function mode, such as reconfigured narrowband to narrowband with harmonic

suppression capability. In addition, the application of harmonic suppressed feature in an reconfigurable antenna is getting an attractive attention since it is producing a unique operation and practical in size. In the first stage of work, there is a need to design an antenna with this feature by integrating a filter to provide the most optimum antenna performance. Employing the HSA can simplify the RF front-end circuit as well as to reduce the EMI in this unit. Furthermore, a compact radio frequency front-end unit can be developed. The conventional HSA structure consists of the antenna with an external low pass filter (LPF) which acts as a 'frequency tuner' to reject the unwanted harmonic frequency. Since the structure employed this tuning circuit, an additional insertion loss is generated. As far as the reconfigurable structure is concerned, the advanced feature provides a significant advantage over an existing reconfigurable antenna.

In this research, a small single band dipole antenna is proposed with tunable features of a practically compact size. The work focuses on two sets of antennas; harmonic suppressed fractal dipole antenna and harmonic suppressed reconfigurable fractal dipole antenna. No such work has been reported in the literature.

1.3 Research Objective

The objective of the research is:

(1) To design and develop fractal dipole antenna with tapered balun

(2) To design and develop harmonic suppressed fractal dipole antenna with tapered balun

(3) To design and develop harmonic suppressed reconfigurable fractal dipole antenna with tapered balun

1.4 Research Scopes

The scopes of works including the design of the antenna, the simulation process, fabrication, measurement and analysis the data. In this work, the aim of the final design is producing the antenna with an optimum structure and performances.

The proposed antenna is designed based on the related microvawe theory equations for a user terminal application. The target frequency is 0.9 GHz since it is in ultra high frequency (UHF) band. The antenna design has been drawn by using AutoCAD software, and then simulated by using commercial software called CST (Computer Simulation Technology) and HFSS (High Frequency Simulation Surface), respectively. In the simulation study, the parameters of antenna have been identified. The fabrication of this antenna has been made by using dry etching technique. A tunable conventional printed dipole antenna with harmonic suppression capability has been successfully designed based on [17]. It employs rectangular gaps as ideal switches, but fabricated on low cost lossy material. Based on this, two sets of antennas are proposed; harmonic suppressed antenna and harmonic suppressed reconfigurable dipole antenna. Both antennas employs Koch curve as a radiating element in order to miniaturize the antenna size. In addition, an open circuit stub is employed to eliminate higher order modes. Ideal switches are also employed to vary the radiating length, thus featuring the tunability characteristic.

In the preliminary research, the work in [17] is referred for the design of a fractal dipole antenna aiming for investigating its frequency reconfigurability characteristics. The design is extended on low loss material, Rogers RT/Duroid 4350B. The antenna operates as 0.9 GHz single band fractal antenna. A scattering parameter analysis is done for the radiating element, stubs and balun, and the tunable antenna. A broadband balun of linear transition with reduced size is employed. The latter can provide highest impedance matching [18] to cater for future demands. To minimize the whole design, an integrated balun-stub is proposed and the final size is practical enough for a handheld unit.

Similar steps are taken to design the active fractal dipole antenna with the same specification. Two commercial softwares are used for simulating the antennas.

The proposed antennas have three unique features i.e. miniaturization, tunability and harmonic suppression capability. Since the reconfigurable antenna is a promising candidate to be used in CR system, the antenna designed in this work is based on a system scenario. The configuration can avoid adjacent channel interference. The controllable frequency of fifteen bands within 400 MHz to 4000 MHz. The antenna will select a single microwave band at a time and suppressed the unwanted higher order modes simultaneously are the main feature of the proposed antenna.

1.5 Significance of Research Contribution

The significance of research contributions are as follows.

(i) The implementation of fractal Koch curve has improved the dimension of the antenna size by reducing the radiation element for frequency variable printed dipole antenna (operation range from 900 MHz to 3.5 GHz) with the ability to suppress harmonics. The configuration is proposed since it exhibits omni-directional radiation pattern with low level of cross-polarization and has the ability to suppress higher order modes, although with a simple structure. The fractal technology applied allows minimization of the antenna size. Open circuit stub is employed to trap the higher order mode that acts as stub-filters.

(ii) The realization of tapered balun with different sizes on low loss material such as Rogers 4350B contribute to four optimum HSA antennas. The antennas are built based on miniaturized fractal dipole (MFD) antenna, named MFDB antennas. The most optimum antenna with minimum size balun is compared

with a previous work [17] in terms of frequency reconfigurability, size reduction and capability to suppress HMs.

(iii) Finally, the development of a set of tunable harmonic suppressed fractal dipole antennas. These are named as tunable miniaturized fractal dipole or TMFDB antennas. The optimized configuration is fabricated using 50 ideal switches located on the fractal dipole arm as well as on the two parallel stubs. The performances are compared with that of [17] in terms of tunable bandwidth and switchable frequencies..

1.6 Organization of the Thesis

Chapter 1 presents the background of the research work, problem statement, objectives, scope, and significance research contribution. The organization of the thesis is then given.

Extensive literature study particularly on reconfigurable antenna, miniaturization techniques, harmonic suppressed antenna, and balun system are carried out. These are presented in Chapter 2. These topics are needed for designing an optimum harmonic suppressed antenna. To achieve such antenna, the fractal curve is selected. Typical techniques to suppress the harmonics in the antenna are given. The conventional printed dipole antenna is used as the basis structure in order to develop a new harmonic suppressed antenna design.

One set of harmonic suppressed fractal dipole antenna and its tunable configuration; implemented on a low cost lossy material (FR-4) has been proposed and tested. This is elaborated in Chapter 3. With in depth analysis and study, the results obtained help to identify and fulfill a gap of research on the typical available reconfigurable antenna, hence the new structure are successfully done in the following works.

In Chapter 4, four sets of wideband tapered baluns (linear transition) with reduced size have been designed and tested. These are then used as the feed line for the developed antennas. Two sets of fractal dipole antennas integrated balun with reduced size (four sets for each group) are developed and tested to study the antenna with different types of tapered line feed.

Chapter 5 presents the design, simulation and development of four sets of harmonic suppressed fractal dipole antennas with reduced size named MFDB. The antennas have an advanced feature by means of harmonic suppression capability. The proposed antenna has a unique structure compared harmonic suppressed antennas available in the literature.

Chapter 6 presents the design, simulation and development of the harmonic suppressed fractal dipole antennas with reduced size named TMFDB. These are extended designs described in Chapters 3 and 5. The antennas are designed and studied using an ideal switch. The results show that the integration of the stubs-filter has insignificant impact on degrading the antenna performances. This proposed reconfigurable antenna has a unique structure compared to similar functioning antennas available in the literature. An active TMFDB25 antenna with four bands is developed by enhancing the performance of RF PIN diodes, DC line, RF choke and DC blocker. The design is limited from 400 MHz to 2.0 GHz.

Finally, Chapter 7 concludes the thesis and suggested future works.

CHAPTER 2

LITERATURE REVIEW

2.1 Review of Reconfigurable Antenna

Latest approaches of reconfigurable antenna designs for wireless system applications are reviewed in this section. There are at least four different classes of antennas, based on different applications. The first is the "multiband tunable". The antennas are designed to have tunability in each operating band, employing more than one radiating element controlled by varactor diodes. Typical application is for user terminal. The design aims to allow the terminal to scan the frequency in each band, and to have a capability to switch to another band if desired.

The second class is the "narrowband tunable". The antennas are designed as scanner and RF communication through certain frequencies. The design aims to scan the frequency in a wideband range using a narrowband channel at any given time. Typical designs use single radiating element.

The third class is the "wideband tunable". The antennas are designed as wideband scanner and broadband RF communication. The antennas use broad

bandwidth for RF communication at any given time through wideband antenna, an array structure, or log periodic structure. The RF switches are used to control the radiating elements with broadband responses.

The final class is the “integrated wideband/tunable narrowband”. The antenna uses two ports or two different feedings for two different antennas. The wideband antenna aims to scan the frequency in wideband range while the RF communication is achieved through a tunable narrow band antenna.

Thus, a “modern” reconfigurable antenna for a user terminal must be optimized with tunable characteristic. Its properties include tunable range, radiation pattern, antenna matching, size, complexity and requirement for harmonic suppression capability.

2.1.1 The State of the Art in Antennas Design for User Terminal

Recent market place for smart radio technologies is CR/SDR. This is due to the fact that it promises on cost reduction, improved utilization of spectrum frequency and better quality of services (QoS). In addition, it provides high immunity against electromagnetic interference (EMI). It is expected that future user terminal will use duplex system (cellular radio) and simplex system (TV band) that operates in the UHF band, cellular radio band, and ISM band. As the architecture is user terminal, information is transmitted or received by an omni-directional tunable antenna. A computational intelligent (CI) will perform spectrum sensing tasks which are capable to “sense”, “learn” and “adapt”, work together with the Field Programmable Gate Array (FPGA) board, frequency agile RF front-ends unit and antenna, in order to transmit and receive data through the RF communication.

Antennas for a user terminal are designed to fulfill its design specifications. Typical requirements are that they must radiate omni-directional pattern with tunable narrowband for wide frequency range, and have compact size. An acceptable frequency is from 400 MHz to 4000 MHz. They must be well matched (i.e. achieve VSWR < 2) to the frequency agile RF front-ends unit of transmitter and receiver (Tx/Rx). Finally, the CR antenna should be cost effective for mass productions without affecting its performance.

2.1.2 Small Element "Modern" Tunable Antenna

In the previous section, different reconfigurable antenna classes are presented. The proposed research is based on reference [17], refers to the capability of the antenna to suppress harmonic frequency. Besides, the architecture access system reported in [2] and [3] are used to understand the proposed antenna concept.

In early 2000, a tunable microstrip antenna was first proposed. Current research on antenna is focused on a vivaldi antenna, mono circular disc antenna, planar inverted-F antenna (PIFA), rectangle patch antenna (used parasitic elements), log periodic dipole antenna (LPDA), microstrip patch array or integrated two antennas using two feed points to reconfigure frequency without degrading its radiation pattern properties. The antennas have the advantages and disadvantages with respect to their use i.e. in user terminal application. It is known that one limitation of a microstrip antenna is its fixed frequency characteristics, with narrow bandwidth of approximately 1 to 3% that are common for antenna elements such as dipole, monopole or a slot. Advances of semiconductor technology on RF switches allow their integration into the antenna, thus embedding the tunable feature. Among them are given in Figures 2.1 to 2.3.

Reported reconfigurable dipole antennas in [23]-[24] are active dipole antenna, and dual band dipole antenna which have a capability to change the operating frequency. The former antenna used four PIN diodes to make three

different segments allowing the antenna to reconfigure at 5.2 GHz, 5.5 GHz, and 5.8 GHz, respectively while the latter antenna employed two MEMS switches to change the frequency of 9 GHz and 4.88 GHz. Figure 2.1 depicts examples of reconfigurable dipole antennas.

A proposed reconfigurable dipole antenna using four reactive loads on a dipole arm is depicted in Figure 2.2(a)[25]. It can configure six operating frequencies from 50 MHz to 350 MHz. Eight switches are placed on the parasitic element that is located in the folded dipole antenna [26]. The configuration has 5 different states, as presented in Figure 2.2(b). Reconfigurable Vee antenna with MEMS shown in Figure 2.2(c) is a printed dipole antenna using a dynamic actuator which can alter its radiation characteristics [27]. MEMS actuators can change the geometry of the dipole. Vee angle is altered when the actuator push-pull on the dipole arm is activated. Vee actuators are symmetrical, producing a variety of angles, hence will produce wider or narrower main radiation beams and can thus be steered. The three layer antenna is constructed using a polysilicon surface micromachining process. It is demonstrated at 17.5 GHz that has an ability to produce the configuration at another frequency. The antenna shows the main radiation is shifted to 48°.

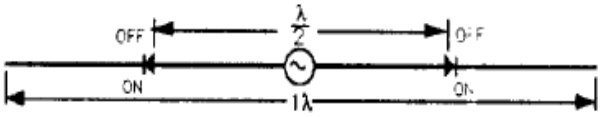

(a)

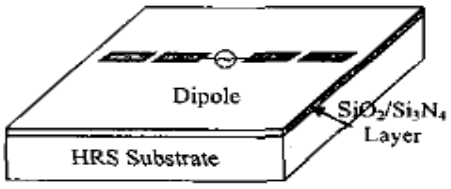

(b)

Figure 2.1 Reconfigurable dipole antenna (a) printed dipole using pin diode [23], and (b) printed dipole using MEMS switches [24].

(a)

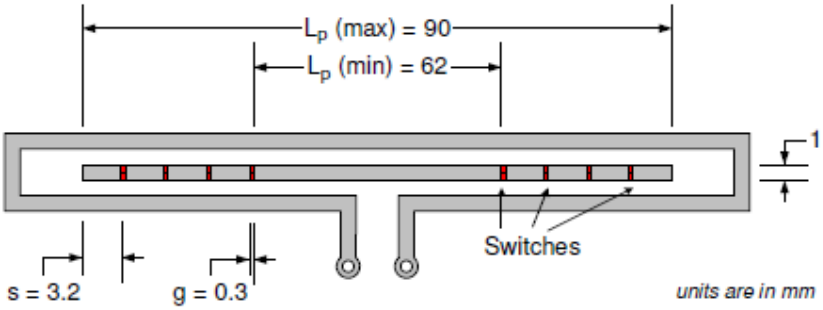

(b)

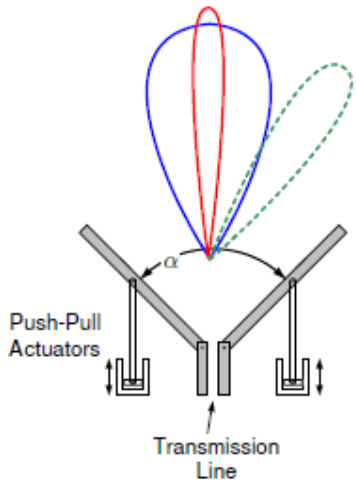

(c)

Figure 2.2 Frequency reconfigurable dipole (a) [25] using linear dipole (b) [26] using a folded dipole, and (c) [27] using a vee-dipole.

Narrowband to narrowband reconfigurable dipole antenna with harmonic suppressed can be demonstrated by using a switch that switches ON and OFF the radiating element. A stub with different length can be used to suppress the harmonic frequency. The work on this type of antenna has been reported, but using a linear dipole and log periodic dipole array as illustrated in Figure 2.3. The first idea to

create such antenna is presented in [17]. In a reconfigurable linear dipole, switches are used to control the antenna and the stub length. The antenna can change the operating frequency from a narrowband to narrowband features as well as suppressed the harmonic frequency in the frequency range of 900 MHz to 3.5 GHz. However, this antenna is large due to the antenna itself as well as the tapered balun used. Meanwhile, the second antenna demonstrated by using the log periodic array [28]. It can configure the operating frequency i.e. from wideband to narrowband, by switching ON and OFF the radiating elements. Ideal switches are also used to control each pair of dipole arm and to switch the related stub. Moreover, the antenna can work from 1 to 3 GHz and can be changed to other narrowband frequencies but with large size.

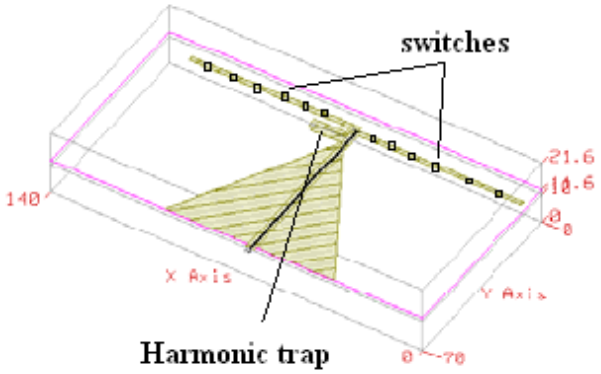

(a)

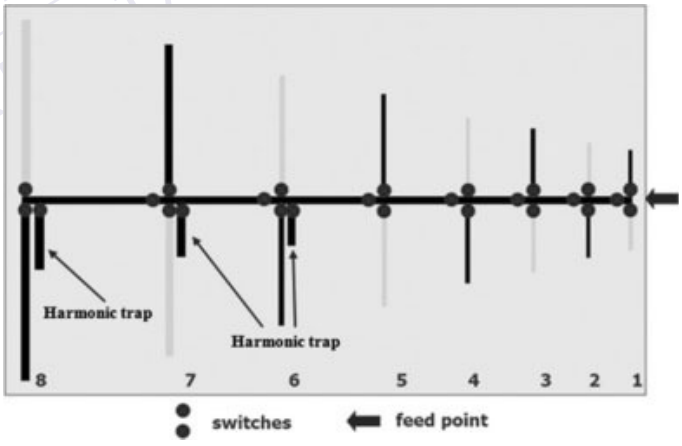

(b)

Figure 2.3 Harmonic suppressed reconfigurable dipole antenna (a) [17] using a linear dipole, and (b) log periodic antenna [28].

2.1.3 Tuneability Technique

Switching ability is a concept for tunable antenna. Three methods have been reported to configure an antenna by means of PIN diode, MEMS switches or external tuner. The effects are either changing the bandwidth, radiation pattern or antenna polarization. The reconfigurable antennas can be conditionally divided based on switching technique [5]. It is proposed that the tunable antenna is a potential candidate for CR application. The methods are:

(i) *Pin diode and GaAs FET:* Pin diode and GaAs FET can be used as switches in reconfigurable antenna, albeit some drawbacks. Pin diode has advantages such as (i) better reliability, (ii) faster in switching speed, (iii) low applied voltage, (iv) broadband frequency switching, (v) easy to integrate with patch antenna, (vi) polarization diversity, (vii) low loss and low cost. Its drawbacks include poor RF performance (insertion loss, isolation loss, etc.), narrow bandwidth and small operational frequency range. GaAs FET offers lower consumption with poor linearity and high loss. Detail discussion on pin diode switches are given in [4], and [6]. Applying reconfigurable antenna for CR antenna system is proposed in [4]. The system consists of tunable microstrip antenna which can be tuned from 1.36 GHz to 1.92 GHz using 13 switches with parasitic patches. The microstrip patch antenna with slits has been used to control the first resonance frequency in a dual band equilateral-triangle microstrip antenna while maintaining its second band [6].

(ii) *MEMS switches:* MEMS switch technology offers high performance due to small insertion loss, low loss, low power consumption, wide bandwidth, and allows beam steering. However, MEMS holds some unattractive disadvantages such as high operating voltage and high cost with low reliability. MEMS switches application is discussed in [29]-[32]. Two MEMS switches are used in a multiband antenna to switch frequency bands, WWAN (fifth band) and WLAN frequency (dual band) [29]. Spiral tightness in rolled planar monopole can be used to change the frequency from 2.2 GHz to 15 GHz [30]. A dual band Yagi patch antenna with three switches to switch bands covering from 9.15 to 9.45 GHz, from 10.3 to 10.45 GHz with controlled beam direction and configured radiation pattern [31]. An array

antenna which uses 9 switches to switch the beam direction up to 40 GHz is discussed in [32].

(iii) *External tuner:* Varactor diode performs as frequency band tuner and work together with external tuner. It provides continuous reactive tuning but with poor linearity characteristics [33] - [34].

In this research, an ideal RF switch by means of gap (simulation) or hard core wire (measurement) are used to tune the antenna's operating frequency. The technique has been well used in [5], [17] and [28]. In this study, the switch design methodology is discussed in Chapter 3 while the comparisons among available switches are also described briefly in this chapter. One prototype of the antenna is demonstrated using a real PIN diode in Chapter 6. Some of antennas in this section are summarized in Table 2.1.

Various methods may be used to produce the frequency reconfigurable antenna as described. However, this antenna can only change the frequency without having the proposal to reduce the size and offer an additional feature. The table has separated the antennas into three groups, (i) antenna using ideal switches, (ii) antenna that uses a high number of ideal switches, and (iii) antenna using a PIN diode switches. These demonstrate such antennas using ideal switches while the use of PIN diodes is preferred. The design of reconfigurable antenna is referred to the application either for a user terminal or based terminal. Frequency reconfigurable antenna can be changed either a narrowband to narrowband, narrowband to wideband or vice versa, or wideband to wideband operation. The configuration of a narrowband to narrowband with harmonic suppression has a potential to be used for a wireless radio application. Similar use of ideal and PIN diodes are employed in the proposed designs presented in the thesis.

Table 2.1: reconfigurable printed antenna

Ref	Authors	Antenna Structure	Switching Band	Frequency Switching Technique	Switch types	Number of switch
[42]	A. Eldek *et al.* (2011) (Jackson State University, USA)	double-dipole	multiband and broadband works at 1.85 GHz, 2.16 GHz, 2.4 GHz, 2.5 GHz,	controlling effective radiating length	metal patch (ideal switches)	4
[43]	V. Zachou *et al.* (2006) (Universiti of New Mexico, USA).	double-sleeved monopole antenna	Mode 1: 2.46 GHz, 2.89 GHz, and 3.33 GHz Mode 2: 2.65 GHz and 3.09 GHz	controlling the parasitic element to vary the effective radiating length	metal patch (ideal switches)	4
[44]	A. H. Ramadan *et. al* (2009) (American University of Beirut, Lebanon)	U-slotted Koch Patch	Mode1: 1.9 GHz & 2.7-6.6GHz Mode2: 2.1 GHz & 2.4 – 6.7 GHz Mode3: 2.5 GHz – 6.7 GHz	controlling effective radiating length	metal patch (ideal switches)	10
[45]	J. Costantine *et al.* (2007) (University of New Mexico, USA)	hexagonal patch	Mode1: 3 GHz and 4 GHz Mode2: 4 GHz and 5 GHz Mode3: 3.5 GHz to 3.8 GHz & 43 GHz to 4.7 GHz	parasitic element	metal patch (ideal switches)	6
[46]	F. Yang and Y. R. Samii (2005) (Univ. of California, USA)	patch with the slot	Mode1: 4.38 GHz Mode2: 4.82 GHz	switchable slot	PIN diode	2
[47]	K. Sakamoto *et al.* (2005) (Saga University, Japa	patch with rectangle slot	Mode1:3.43 GHz Mode2: 3.1 GHz	switchable slot	PIN diode	2
[26]	N. P. Chamming (2003) (Virginia Polytechnic Institute & State University	PIFA	1.48 GHz, 1.49 GHz, 1.5 GHz, 1.51 GHz, 1.53 GHz, and 1.51 GHz, and 1.54 GHz. They are affected on the BW reconfigurable	changing the ground plane length	metal patch (ideal switch)	12
[26]	N. P. Chamming (2003) (Virginia Polytechnic Institute & State University	RRPA	1.50 GHz, 1.52 GHz , and 1.53 GHz. They are affected on the BW reconfigurable.	Controlling the ring width.	metal patch (ideal switch)	80

(Contd.)

[26]	refer to Figure 2.2 (b) N. P. Chamming (2003) (Virginia Polytechnic Institute & State University	RPFDA	0.94 GHz, 1.01 GHz, 1.03 GHz, 1.04 GHz, 1.05GHz, 1.12 GHz. They are affected on the BW reconfigurable.	Controlling the parasitic element length.	metal patch (ideal switch)	8
[48]	A. Sondas *et al.* (2012) (Kocaeli University, Turkey).	loop-loaded dipole	Mode1: 2.8 – 3.2 GHz Mode2: 4.9 – 5.6 GHz	controlling effective radiating length using a parasitic element	PIN diode	2
[49]	-*W. S. Kang et al. (2008)* (Yonsei University, Korea)	linear dipole	Mode1: 2.35 GHz Mode2: 2.64 GHz	Controlling effective radiating length	PIN diode	3
[50]	I. Tekin and M. Knox (2012) (Sabanci University, Turkey & Polytechnic Institute of NYU Brooklyn, New York)	two patches with slot	Mode1: 2.4 GHz Mode2: 5.6 GHz	switching either from patch 1 to patch 2 or vice versa	PIN diode	4
[17]	refer to Figure 2.28 (b) A. Mirkamali *et al.* (2006) (University of Birmingham, UK)	Linear dipole	0.9 GHz, 1.05 GHz, 1.205 GHz, 1.460GHz, 1.750GHz, 2.05GHz, and 2.770GHz.	controlling effective radiating length	metal patch (ideal switch)	24
[28]	refer to Figure 2.28 (b) A.Mirkamali *et al.* (2010) (University of Birmingham, UK)	Log periodic dipole	Mode1: 1-3 GHz, Mode2: 0.94 GHz, Mode3: 1.217 GHz Mode4: 1.477 GHz	controlling effective radiating element	metal patch (ideal switch)	28

2.2 Review of Fractal Antenna

Since the introduction of the Koch curve [56], many new and unique antenna configurations have been reported. Compact size and high performance antenna are desired in many of today's telecommunication system to reduce the cost and minimize the size of the system device. The planar fractal dipole antenna was studied extensively [93], and [94]. Other than the Koch curve, Minskowski, Sierpinski, and Hilbert curves are fractal patterns. In this research, the Koch curve is selected due to its ability to reduce the antenna size and increase its operating bandwidth. Besides that, the antenna has a simple structure and robust construction.

Most of the research on fractal dipole antenna concentrates on the antenna design and its corresponding characteristics. As far as the Koch dipole is concerned, designs reported in the literature used a single-sided configuration which is needed for a complicated balun circuit. The input impedance of fractal was addressed in designing the feeding circuit [54]. An expression of the input impedance of Koch dipole is also presented [60]. A Koch fractal monopole is one of the earlier designs of fractal antennas. Both reported antennas experienced size reduction with multiband characteristics. On the other hand, the implementation of fractal Koch in a dipole antenna allows size reduction while increases the numbers of higher modes frequencies [95]. The miniaturisation of the antenna by employing the Koch curve is discussed further in chapters 4 and 5.

A critical characteristic for fractal antenna is the input impedance. It is lower than the conventional printed dipole antenna with respect to the number of iteration, *n*. By changing *n* of the Koch curve antenna, the fractal dimension changes as well as the input impedance. It can be observed from the literature that there is a relationship between fractal variation and antenna performance. It is expected that the employed idea will significantly realized for fractal dipole antenna designs. In this study, the investigation carried out is to integrate the double-sided Koch dipole with a feeding system to allow the antenna to practically operate as depicted in Figure 2.4. Since the operating frequency is the main target, *n* is limited to 2 and indentation angle is 60°. This is because, comprehensive works performed by other researchers on the characteristics of fractal dipole antenna are in terms of indentation angle, *n* and the operating frequency.

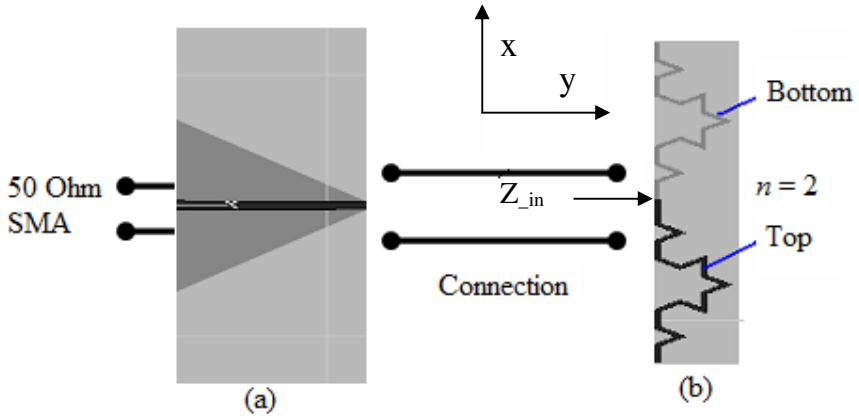

Figure 2.4 (a) Tapered balun, and (b) Input Impedance, $Z_{in\text{-}antenna}$ of printed Koch dipole antenna

For future wireless applications, attractive feature can be incorporated into the dipole antenna such as small physical size. In other words, the designed antenna is practical in size for handheld unit applications as well as can provide better gain and efficiency.

There are various printed dipole antennas integrated with balun for omni-directional applications [96]–[100]. A 2.4 GHz printed dipole antenna was reported together with a microstrip via hole transition that act as a balun [96]–[97]. Measured bandwidth of 30% (for VSWR < 2) presents an advantage of the balun [98] and the ground plane is changed to V-shape to broaden the bandwidth. The modified marchand balun is used for dual 900 MHz/2 GHz wideband printed dipole [99]. A typical tapered balun is used for 2.4 GHz printed dipole antenna [100]. However, most of these antennas use a complicated tapered balun and the size is big. To achieve the research objective, double-sided fractal dipole antenna integrated with a tapered balun is developed. This structure has a capability to trap the higher order modes (discussed in chapters 5 and 6) and can be easily constructed using tapered balun as a practical matching circuitry. The completed work of the balun size reduction is given in chapter 3.

2.2.1 Koch Curve Properties

The standard Koch curve geometrical construction is shown in Figure 2.5. It is a fairly simple and straight forward design. Initially, the straight line (n = 0) is termed the initiator. n = 1 is termed the generator. It is achieved by partitioning the initiator into three equal parts and replacing the middle segment with two others of the same length at certain angle. The method is repeated for the next generation of n = 2, 3 and 4. It is interesting to note that the first iterated curve is 1/3 from the original length. Furthermore, the curve has four segments when n = 1. Therefore, for n^{th} iteration the unfolded length is $\left(4/3\right)^n$. This feature is the key to the development of the antenna design.

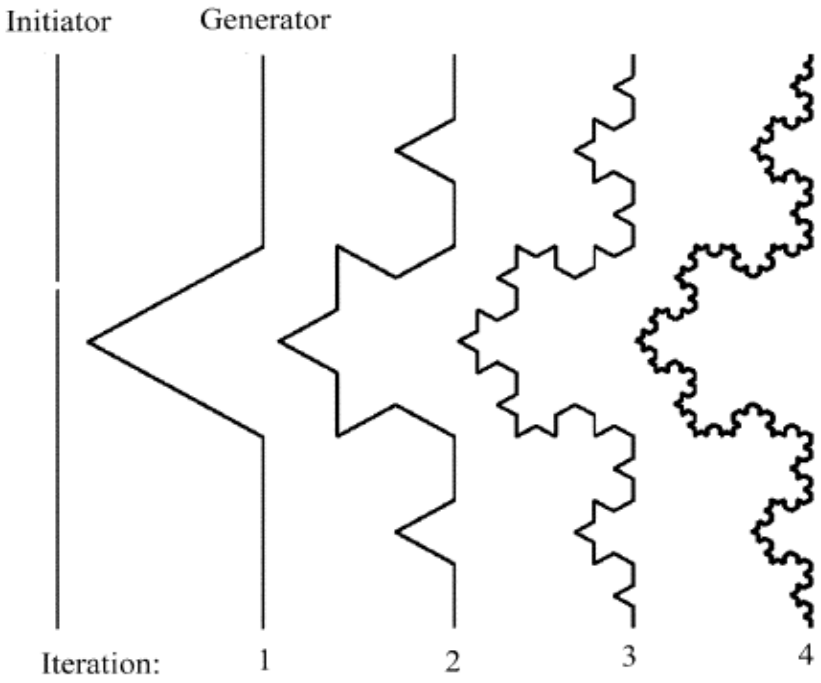

Figure 2.5 Fractal Koch's geometries construction [54]

The iteration function system (IFS) shown in Figure 2.6 is used for generating the standard Koch curve. They are represented by a set of affine transformations

forms. It is assumed that the original unit length is located at the x-axis. The generated segments are found by the expression given next.

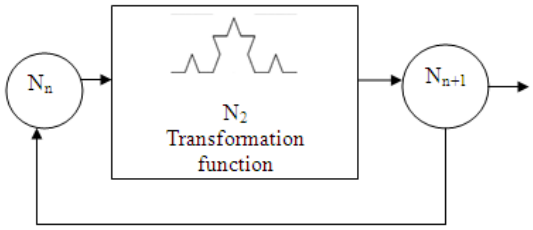

Figure 2.6 Block diagram of the IFS [54]

The Koch curve iterated function system is given by [54]

$$W(x,y) = W_1(x,y) \cup W_2(x,y) \cup W_3(x,y) \cup W_4(x,y) \tag{2.1}$$

where

$$W_1\begin{pmatrix} x' \\ y' \end{pmatrix} = \begin{bmatrix} \frac{1}{3} & 0 \\ 0 & \frac{1}{3} \end{bmatrix} \begin{pmatrix} x \\ y \end{pmatrix} \tag{2.2}$$

$$W_2\begin{pmatrix} x' \\ y' \end{pmatrix} = \begin{bmatrix} \frac{1}{3}\cos 60^o & -\frac{1}{3}\sin 60^o \\ \frac{1}{3}\sin 60^o & \frac{1}{3}\cos 60^o \end{bmatrix} \begin{pmatrix} x \\ y \end{pmatrix} + \begin{pmatrix} \frac{1}{3} \\ 0 \end{pmatrix} \tag{2.3}$$

$$W_3\begin{pmatrix} x' \\ y' \end{pmatrix} = \begin{bmatrix} \frac{1}{3}\cos 60^o & \frac{1}{3}\sin 60^o \\ -\frac{1}{3}\sin 60^o & \frac{1}{3}\cos 60^o \end{bmatrix} \begin{pmatrix} x \\ y \end{pmatrix} + \begin{pmatrix} \frac{1}{2} \\ \frac{1}{2}\sin 60^o \end{pmatrix} \tag{2.4}$$

$$W_4\begin{pmatrix} x' \\ y' \end{pmatrix} = \begin{bmatrix} \frac{1}{3} & 0 \\ 0 & \frac{1}{3} \end{bmatrix} \begin{pmatrix} x \\ y \end{pmatrix} + \begin{pmatrix} \frac{2}{3} \\ 0 \end{pmatrix} \tag{2.5}$$

The corresponding curve iteration construction is the Koch fractal dipole (i.e. n = 0, 1, 2, 3, etc.). This process is repeated for all higher iterations of the geometry.

It may be observed that the straight line distance between the start and end points of all iterations is the same. In addition, the scale factors and rotation angles in these transformations are such that they lead to a self-similar geometry, a visually apparent fact. The similarity dimension of the geometry can thus be calculated as [54]:

$$D = \frac{\log 4}{\log\left(2(1+\cos\theta)\right)} \tag{2.6}$$

When θ = 60°,

$$D = \frac{\log 4}{\log 3} = 1.26186 \tag{2.7}$$

It is found that from the calculation, when the angle is 60°, four initial lengths are reduced by 3. In other words, the dimension Koch antenna is increased by a factor of 1.26 compared to the initial.

2.2.2 Reconfigurable Fractal Antenna

Reconfigurable fractal antennas have attracted many researchers in recent years [51]-[57]. The antenna has many advantages such as large bandwidth, multi-frequency and can reduce the antenna size of Koch and Hilbert curves as well as a Sierpinski Carpet. It is among the selected geometry to be studied for the antenna innovation. Many researchers have used these geometries in order to generate reconfigurable antenna that can configure the frequency or radiation pattern with size reduction. Figure 2.7 presents typical fractal curves.

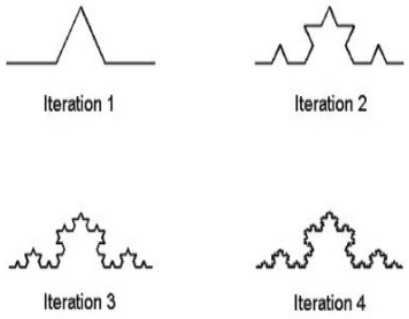

(a)

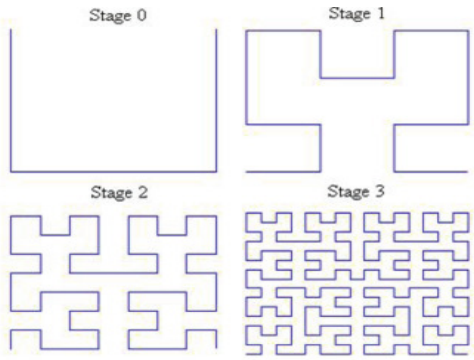

(b)

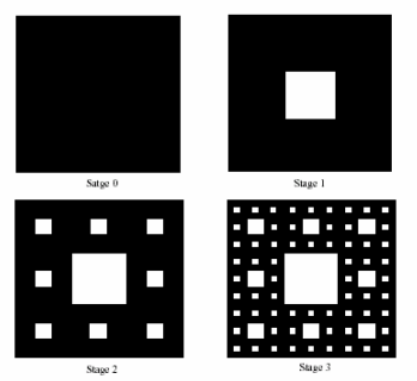

(c)

Figure 2.7 Typical fractal curve. (a) the first four iterations in the construction of a stand Koch curve, (b) the first four stages in the construction of a Hilbert curve, and (c) the four stages in the construction of Sierpinski Carpet curve.

A Hilbert curve patch antenna uses six MEMS switches to configure the radiation pattern from 12.4 GHz to 12.65 GHz [51]. Four MEMS switches are used

in a Sierpinski Gasket dipole to switch the operation from 14 GHz (band 1) to 8 GHz and 25 GHz (band 2) [52]. Other similar studies use Sierpinski gasket, Hilbert curve and von Koch geometry [53]-[58]. Three switches are located at the radiating element to change the operating frequency at 620 MHz, 630 MHz, and 640 MHz [53]. Five states of operating frequency in Sierpinski Gasket's antenna by controlling the switches condition are demonstrated [54]. Twelve switches are used to tune 60 GHz and 80 GHz in the Koch patch antenna [55]. Thirty switches are used in three dimensional fractal tree antennas to configure the operating frequency from 770 MHz to 1570 MHz [56]. Six switches are employed in a Sierpinski Gasket antenna to tune the frequency at 2.4 GHz, 5.7 GHz, 9.4 GHz, and 18 GHz [57]. Four switches are used to configure the radiation pattern at 8.4 GHz in a square patch fractal [58]. Some of them are summarized in Table 2.2.

Table 2.2: Reconfigurable fractal antenna

Reference	Antenna Structure	Number/Type of Switches	Comments
[57]	Sierpinski Gasket	6/ MEMS switch	changed the frequency from 2.4 GHz, 5.7 GHz, 9.4 GHz to 18 GHz.
[52]	Sierpinski Gasket	4/ MEMS switch	changed the frequency from 7 GHz, 8 GHz, 14 GHz to 23 GHz
[56]	Fractal tree	204/copper strip (ideal switch)	changed the frequency from 600 MHz to 1600 MHz (approximately 20 bands)
[53]	Hilbert curve	2/metal patch (ideal switch)	changed the frequency from 620 GHz, 627 GHz, to 635 GHz.
[51]	Hilbert curve	8/ metal patch (ideal switch)	changed the pattern at 12.4 GHz to 12.65 GHz
[55]	Koch Patch	18/copper strip (ideal switch)	changed the pattern at 60 GHz and 80 GHz
[58]	Square fractal loop	4/metal patch (ideal switch)	changed the pattern at 8.4 GHz

2.3 Review of Antenna Miniaturization

Antenna miniaturization is needed to ensure the designed antenna is practical for wireless system applications. There are several possible reported techniques such as using fractal curve [59]–[60], meandering line [61]–[62], superconducting material [63], low temperature co-fired ceramic, LTCC material [64]–[66], slotted

APPENDIX F

PUBLICATIONS DURING THE DOCTORATE STUDY

1. S. A. Hamzah, M. Esa, N. N. N. Abd Malik, and M. K. H. Ismail. Narrowband-to-Narrowband Frequency Reconfiguration with Harmonic Suppression using Fractal Dipole Antenna. International Journal of Antenna and Propagations (Accepted 2 July 2013). pp 1-8. IF = 0.683.
2. S. A. Hamzah, M. Esa, N. N. N. Abd Malik, and M. K. H. Ismail.Tapered Balun Design for a Meander Fractal Dipole Antenna with Reduced Size. Turkish Journal of Electrical Engineering & Computer Sciences (date of revised manuscript submission: 22 April 2013). pp 1-11. IF = 0.2
3. S. A. Hamzah, M. Esa, N. N. N. Abd Malik, and M. K. H. Ismail. Small Size Koch Fractal Dipolea Antenna Integrated with Harmonic Suppression Capability. Jurnal Teknologi, Universiti Teknologi Malaysia (date of submission: 31 January 2013). pp 1-10. SCOPUS Indexed.
4. S. A. Hamzah, M. Esa, N. N. N. Abd Malik, and M. K. H. Ismail. Switchable Fractal Dipole Antenna with Harmonic Traps. Electronic Letter (date of submission: 30 December 2012). pp 1-2. IF = 0.965
5. S. A. Hamzah, M. Esa, N. N. N. Abd Malik, and M. K. H. Ismail. Design of Harmonic Suppressed Reconfigurable Fractal Dipole Antenna. PIER (date of submission: 26 October 2012). pp 1-18. IF = 5.298
6. S. A. Hamzah, M. Esa, N. N. N. Abd Malik, and M. K. H. Ismail. Harmonic Suppressed Fractal Dipole Antenna with Reduced Size. PIER (date of submission: 05 October 2012). pp 1-16. IF = 5.298

7. S. A. Hamzah, M. Esa, N. N. N. Abd Malik, and M. K. H. Ismail. Reduced Size Harmonic Suppressed Fractal Dipole Antenna with Integrated Reconfigurable Feature. A special issue at the International Journal of Multimedia Processing and Technologies (JMPT), vol. 2, no. 1, pp. 55 – 65 (March 2011).
8. S. A. Hamzah, M. Esa, N. N. N. Abd Malik, and M. K. H. Ismail. Frequency Reconfigurable Koch Fractal Dipole Employing Harmonic Traps. The 2013 Asia-Pacific Microwave Conference. APMC 2013, Seoul, Korea. 5 - 8 November 2013.
9. S. A. Hamzah, M. Esa, N. N. N. Abd Malik, and M. K. H. Ismail. Reconfigurable Harmonic Suppressed Fractal Dipole Antenna. The 2012 Asia-Pacific Microwave Conference. APMC 2012, Kaohsiung, Taiwan. 4 - 7 December 2012.
10. S. A. Hamzah, M. Esa, N. N. N. Abd Malik, and M. K. H. Ismail. Broadband Microstrip-to-Parallel Strip Transition Balun with Reduced Size. The 2012 Asia-Pacific Microwave Conference . APMC 2012, Kaohsiung, Taiwan. 4 - 7 December 2012.
11. S. A. Hamzah, M. Esa, N. N. N. Abd Malik, and M. K. H. Ismail. Novel Active Reconfigurable Fractal Dipole Antenna using RF PIN Diodes. The 2011 International Symposium on Antennas and Propagation. ISAP 2011, Jeju, Korea. 25-28 October, 2011.
12. S. A. Hamzah, M. Esa, N. N. N. Abd Malik, and M. K. H. Ismail. Reduced Size Harmonic Suppressed Fractal Dipole Antenna with Integrated Reconfigurable Feature. The 6th International Conference on Signal-Image Technology & Internet Based Systems. SITIS 2010, Kuala Lumpur, Malaysia. 15-18 December 2010.
13. S. A. Hamzah, M. Esa, and N. N. N. Abd Malik. Reduced Size Harmonic Suppressed Microwave Fractal Meander Dipole Antenna with Reconfigurable Feature. The 2010 Asia-Pacific Microwave Conference . APMC 2010, Yokohama, Japan. 7-10 December 2010.
14. S. A. Hamzah, M. Esa, N. N. N. Abd Malik, and M. K. H. Ismail. Exeperimental Investigation of Reconfigurable Harmonic Suppressed Fractal Dipole Antenna. The 2010 International Symposium on Antennas and Propagation. ISAP 2010, Macau, China. 23-26 November, 2010.

15. S. A. Hamzah, M. Esa, and N. N. N. Abd Malik. Reduced Size Harmonic Suppressed Fractal Dipole Antenna with Integrated Reconfigurability. The 2010 IEEE Asia-Pacific Conference on Applied Electromagnetics. APACE 2010, Port Dickson, Malaysia. 9-11 November, 2010.
16. S. A. Hamzah, and M. Esa. Miniaturized Single Band Microwave Fractal Meander Dipole Antenna and its Tunable Configuration. The 2010 IEEE International Symposium on Antennas and Propagation. APS 2010, Toronto, Ontario, Canada. July 11-17, 2010.
17. S. A. Hamzah, M. Esa, and N. N. N. Abd Malik. Low Profile Single Band Microwave Fractal Meander Dipole Antenna with Reduced Size. The 2009 IEEE International Conference on Antennas, Propagation and System. INAS 2009, Johore Bahru, Malaysia.3-5 Dec 2009.
18. S. A. Hamzah, M. Esa, and N. N. N. Abd Malik. Reduced Size Microwave Fractal Meander Dipole Antenna with Reconfigurable Feature. The 2009 International Symposium on Antennas and Propagation. ISAP 2009, October, Bangkok, Thailand. 20-23 October, 2009. (Oral Presentation)
19. S. A. Hamzah, M. Esa, and N. N. N. Abd Malik. Reduced Size Microwave Fractal Meander Dipole Antenna with Reconfigurable Feature. The 2009 International Symposium on Antennas and Propagation. ISAP 2009, October, Bangkok, Thailand. 20-23 October, 2009. (Poster Presentation for Best Student Papers Finalists)
20. S. A. Hamzah, M. Esa, and N. N. N. Abd Malik. Reconfigurability Characteristics of Microwave Fractal Meander Dipole Antenna. The 6th Student Conference on Research and Development. SCORED 2008, Universiti Teknologi Malaysia, Johore Baharu, Malaysia. 26-27 November 2008.